Journal of Materials Chemistry B

Accepted Manuscript

ROYAL SOCIETY OF CHEMISTRY

www.rsc.org/materialsB

Journal Name

RSCPublishing

ARTICLE

Monitoring Layer-by-layer Self-assembly Process of Natural Polyelectrolytes by Fluorescent Bioconjugate with Aggregation-induced Emission Characteristic

Cite this: DOI: 10.1039/x0xx00000x

Received 00th July 2014,
Accepted 00th July 2014

DOI: 10.1039/x0xx00000x

www.rsc.org/

Jingwei Jia[a], Zhengke Wang*[a], Wentao Lu[a], Ling Yang[a], Qingwen Wu[a], Wei Qin[b], Qiaoling Hu*[a], Ben Zhong Tang*[b]

A novel chitosan-based fluorescent bioconjugate (TPE-CS) with aggregation-induced emission (AIE) characteristic is synthesized and used as a fluorescent probe for monitoring layer-by-layer self-assembly process of natural polyelectrolytes. QCM results and contact angle measurement indicate that this AIE active TPE-CS bioconjugate can be assembled with alginate (ALG) through layer-by-layer deposition. Ellipsometry and fluorescence (FL) spectroscopy show an exponential growth of the TPE-CS/ALG multilayer films. Moreover, the exponential relationship between the FL intensity and the number of bilayers, which is in accordance with thickness variation of multilayer films, provides solid evidence for its capacity to monitor the layer-by-layer self-assembly process.

Introduction

Biomaterials initially interact with cells and tissues through their interfaces, therefore the surface properties of biomaterials play a crucial role in their applications in numerous biomedical fields. Surface modification or functionalization has always been a hotspot in biomaterial area and attracted great interests[1-2]. One promising way to functionalize biointerface in a controllable and versatile manner can be achieved by the layer-by-layer (LBL) self-assembly technique[3-4]. This technique is based on the alternate deposition of polyanion and polycation to create polyelectrolyte multilayer films (PEM). The advantages of this technique are mainly the wide choice of molecules, the flexibility and simplicity of construction, and the ability to coat materials with any shape and dimension. The physicochemical properties of multilayer films, including the thickness of nanometric layers, the viscoelastic properties of the coating, the surface charge, contact angle, roughness and topography, can be controlled by changing the nature of polyelectrolytes, the deposition conditions (pH, salt concentration, *etc*.) and the outermost layer of the film[5-8].

To ensure that the assembly process is under control, it is necessary to monitor in situ and in real time for the polyelectrolytes deposition and film growth. Quartz crystal microbalance (QCM) and UV-vis absorption are common methods that have been widely used for monitoring the film growth. QCM measurement allows following the build-up of assembly layers and has thus often been used in the studies of LBL deposition processes[9-11]. Besides the QCM technique, UV-vis absorption is another method that has been widely used for monitoring the film growth [12]. However, for UV-vis spectroscopy, the substrate used for the measurement of absorption must be quartz plate for its good transparency to UV-vis light[13], which limits the utility of UV-vis absorption technique greatly.

Fluorescence (FL) spectroscopy, with its ultrafast speed, high sensitivity and substrate independence, has been extensively used in many biological assays. Nevertheless, conventional FL dyes are incapable to be used for monitoring

the electrostatic multilayer assembly of polyelectrolytes due to the notorious aggregation-caused quenching (ACQ) effect and red-shift of the FL spectra when aggregating. In 2001, an uncommon luminogen system, in which aggregation worked constructively, rather than destructively as in the conventional systems was reported[14]. Since the light emission was induced by aggregate formation, the process was termed "aggregation-induced emission" (AIE). A large variety of AIE molecules have been developed and vast high-tech applications of the AIE effect explored in optoelectronic and sensory systems[15-16]. To date, numerous AIE-based biological probes have been successfully invented[17 - 23], thus dramatically extending the application of FL spectroscopy of AIE fluorogens in biological field. J. K. Jin *et al*.[13] have reported an aminated silole with AIE characteristics physically mixed with polycation for monitoring LBL self-assembly processes of polyelectrolytes. The linear relationship between the FL intensity and the quantity of AIE molecules was confirmed.

In our previous work, a novel fluorogenic probe was synthesized by attaching a large number of tetraphenylethene (TPE) fluorogens to chitosan (CS) macromolecular chains[24]. The resultant TPE-CS bioconjugate shows a unique AIE behavior and does well in long-term fluorescent cellular tracing. In this study, TPE-CS is served as a FL probe and also a polycation to be assembled with polyanion (alginate, ALG). We investigate the LBL self-assembly process of TPE-CS/ALG, trying to prove its capacity to be used for monitoring self-assembly of polycation and polyanion.

Experimental

Materials and reagents

CS (Mv=3.8×10^4) was supplied by the Qingdao Haihui Bioengineering Co. Ltd (Qingdao, China) with 93% degree of deacetylation (D.D). ALG (sodium salt, Mv=5.8×10^4) and other reagents were all purchased from Sinopharm Chemical Reagent Co., Ltd. All reagents and solvents were used without further purification.

^{1}H NMR analyses

TPE-CS was fabricated according to the procedures described in our previous work[24], the molar feed ratio of TPE fluorogens to CS sugar rings was 2 mol %. The degree of labeling (DL) of the TPE-CS was determined by ^{1}H NMR analyses.

Buildup of (TPE-CS /ALG)$_n$ Multilayer Films

The substrates used for the LBL self-assembly were quartz plate, silicon wafer and gold coated crystal used in QCM. They were cleaned by dipping into a freshly prepared H_2SO_4/H_2O_2 (piranha, 7:3 v/v) solution, then rinsed with deionization (DI) water and dried with N_2 flow.

Polyelectrolyte solutions (1 mg/mL) were prepared in 0.5 M NaCl aqueous solution (Panreac), and their pH was adjusted to a certain value by adding 0.1 M acetic acid (Panreac). We set the pH of ALG solution at 5.8, and the TPE-CS solutions at 3.6 and 4.5 respectively, which were denoted as ALG (1 mg/mL, pH 5.8), TPE-CS (1 mg/mL, pH 3.6) and TPE-CS (1 mg/mL, pH 4.5).

The substrates were firstly dipped into the TPE-CS solution for 20 min, then rinsed with DI water which has the same pH as the TPE-CS solution. After rinsing, the samples were blow-dried with N_2 flow. Subsequently, they were immersed into ALG solution for 20 min, then rinsed with DI water which has the same pH as the ALG solution, and dried with N_2 flow. This procedure was repeated until the desired number of bilayers was achieved to prepare the (TPE-CS /ALG)$_i$ multilayer films, i is the number of bilayers.

QCM Measurement

The multilayer build-up was monitored in situ by QCM with dissipation monitoring (Q-Sense E4 system, Q-Sense AB, Sweden). QCM-D has the ability of simultaneously measuring the normalized resonant frequency (Δf/n) and energy dissipation (ΔD) shifts.

The gold coated crystals were cleaned by dipping into a freshly prepared H_2SO_4/H_2O_2 (piranha, 7:3 v/v) solution for very short time (10 s), then rinsed with DI water and dried with N_2 flow prior to the experiments. We started the system with 0.5 M NaCl solution (buffer baseline). Then, the polyelectrolyte solutions were injected into the measurement cell for 20 min at a proper flow rate using a peristaltic pump, beginning with TPE-CS. A rinsing step for 10 min with a 0.5 M NaCl solution was included between the adsorptions of each polyelectrolyte. TPE-CS/ALG multilayer films with different layer numbers were fabricated. All the experiments were conducted at room temperature.

Contact Angle Measurement

Quartz plate was used as the substrate to fabricate the multilayer film for the measurement. The self-assembly process was the same as that described above. The measurement of contact angle was performed with the sessile drop method. The volume of the liquid

droplets was kept constant at 1 μL. All the measurements were independently repeated for 3 times.

Ellipsometry and FL spectroscopy

The thickness of multilayer films was determined in air by a spectroscopic ellipsometer (model M2000D, J. A. Woollam Inc., Lincoln, NE) at an incident angle of 75° within a wavelength range of 300-1700 nm, and calculated from the ellipsometric parameters, D and j, using a Cauchy model. FL spectra of the multilayer films were measured on a Perkin-Elmer LS 55 spectro-fluorometer. All the measurements were independently repeated for 3 times.

Atomic Force Microscopy (AFM)

The surface topologies of multilayer films were analyzed by AFM (SPI3800N, Seiko Instrumental, Japan) in tapping mode in air.

Cell Adhesion and Proliferation

The adhesion and proliferation of renal epithelial cell (293T) on the TPE-CS/ALG multilayer films with different layer numbers and different outmost layer were investigated. Cells were distributed into 6-well plates containing the film-coated quartz plates (5000/well) in a total volume of 2 mL DMEM supplemented. The cells were observed under microscope (Olympus IX81, Japan) after cultured for 3 d.

Results and discussion

TPE-CS

^{1}H NMR spectra of TPE-CS showed that labeling the CS with TPE fluorogens has been successfully done, and the DL of the TPE-CS is 0.83 mol % at a feed ratio 2 mol % (Figure 1).

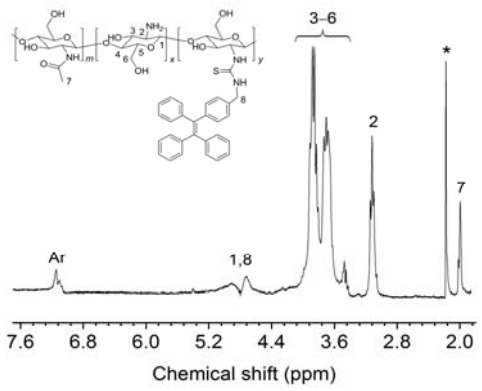

Figure 1 ^{1}H NMR spectra of TPE-CS measured in acetic acid-d_4/water-d_2 mixture at room temperature. The solvent peaks are marked with asterisks.

Optimization of Build-up Conditions for (TPE-CS/ALG)$_n$ Multilayer Films

Both of CS and ALG are weak polyelectrolytes, which are partially charged at moderate pH near their pKa. Thus, the pH and ionic strength are expected to influence film growth greatly. In this research, polyelectrolyte solutions (1 mg/mL) were prepared in 0.5 M NaCl (Panreac). We fixed the pH of ALG at 5.8, and set the pH of TPE-CS at 3.6 or 4.5. QCM-D monitored the build-up of (TPE-CS/ALG)$_3$/TPE-CS multilayer films (Figure 2). The decrease of F after each polymer adsorption step evidenced that mass is being deposited at the crystal surface for both pH conditions (3.6 and 4.5). Also, the sequential deposition process was generally stable and reproducible.

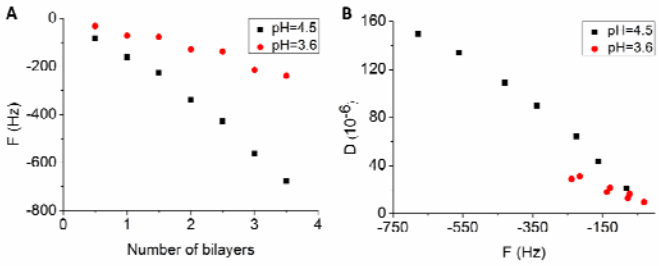

Figure 2 QCM-D results: (A) variation of frequency F with number of layers, (B) variation of the dissipation factor D with frequency F (pH of ALG: 5.8, pH of TPE-CS: 3.6, 4.5).

Since polyelectrolyte deposition is primarily governed by electrostatic interactions, the degree of ionization of the charged molecule is of prime importance[25]. The thickness and organization of these sequentially adsorbed layers are extremely sensitive to the pH of solution since the charge density and conformation of weak polyelectrolytes, like TPE-CS, are influenced by the changes of pH. At pH 3.6, it is expected an increase of the charge density of this weak polycation because lower pH is beneficial for the protonation of the amine groups[26], enhancing electrostatic interactions with the carboxylate groups of ALG. Moreover, the assembled system exhibits a more compact and stiff behavior as a result of a preferential flat conformation[25]. On the other hand, as the pH rises to 4.5, the protonation of amine groups will be decreased, resulting in lower charge density. Thus, there were less amine groups to interact with ALG, therefore, the film structure is more loosely and dissipates more energy. It is already known that polyelectrolyte adsorption is governed by the charge reversal that appears on the film surface after each dipping step and that constitutes the buildup motor for the assembly[22]. When the charge density of the adsorbed species decreased, more

polyelectrolyte chains are needed to overcompensate and invert the surface charge, led to thicker films, which can explain the higher thickness of TPE-CS at pH 4.5 than that at pH 3.6.

Plotting D versus F eliminates the time dependence, and displays how much energy is dissipated by mass adsorbsion (or frequency shift). For the build-up at pH 4.5, the plot's slope is steeper and that indicates a softer and less compact layer is developed. In both condition, data showed that the adsorption of ALG led to higher changes of dissipation, because ALG has a more hydrophilic character than TPE-CS[27]. Due to this water-rich nature (hydrogel like), ALG deposition can be accompanied by solvent entrapment and, hence, resulting in a more viscoelastic multilayered system. And the following adsorption of TPE-CS is accompanied by a decrease in the dissipation due to water extrusion from ALG layer by the electrostatic interactions between the TPE-CS and ALG polyelectrolytes[28]. This phenomenon is much more obvious when the pH of TPE-CS is 3.6 since electrostatic interactions between polyelectrolytes are stronger.

In the following research, we choose the build-up conditions as ALG (1 mg/mL, pH 5.8) and TPE-CS (1 mg/mL, pH 4.5), for the rapid deposition of both polyelectrolytes and inerratic changes of dissipation, which are favourable for the subsequent observation.

Surface Wettability

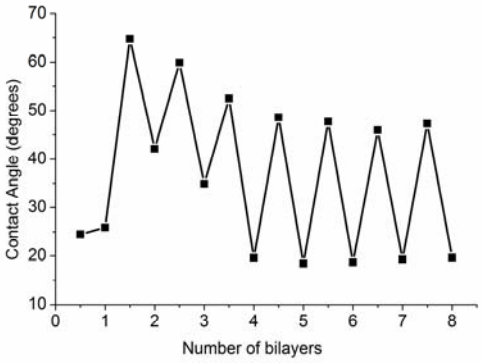

Figure 3 Contact angles of TPE-CS/ALG multilayer films with certain number of layers. Whole numbers represent films with ALG as the outermost layer, whereas half number films have TPE-CS as the outermost layer.

The surface wettability is very sensitive to the surface compositions of the outermost layer. Figure 3 shows the contact angle of the multilayer films with layer number from 0.5 to 8. The contact angles exhibit the zigzag feature along with the changes of layer numbers, indicating that the alternate assembly deposition of TPE-CS and ALG on the surface has been realized. Contact angle of ALG outmost layer is much smaller than that of TPE-CS outermost layer due to the water rich nature of ALG, which is well in accordance with the QCM results. However, the conclusion is not applicable to the first bilayer, because it is so thin of the first bilayer that influence of the substrate is great.

Exponential Growth

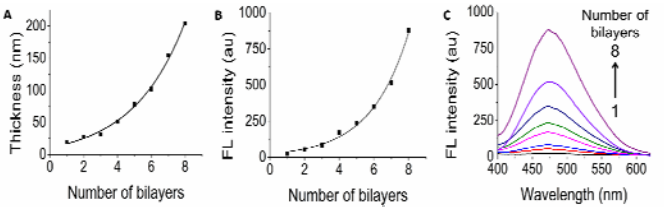

Figure 4 Exponential growth of the TPE-CS/ALG multilayer films: (A) variation of thickness with bilayer numbers, and (B) variation of FL intensity with bilayer numbers. (C) FL spectra of TPE-CS/ALG multilayer films with bilayer number from 1 to 8.

Both ellipsometry and FL are used for measuring the self-assembly deposition of polyelectrolytes multilayer films (Figure 4), which show an exponential growth of the TPE-CS/ALG system. This kind of exponential growth could be explained with a model based on an "inward" and "outward" diffusion process, throughout the entire film, at least one of the polyelectrolytes that comprise the multilayer[29-31]. Specifically, when a film that has been terminated by ALG layer is brought in contact with TPE-CS solution, polycations (TPE-CS) diffuse throughout the entire multilayer film down to the deposition substrate. During the rinsing step, some of these polycations diffuse "out of" the film. Polycations that remain in the film, after rinsing, diffuse "out of" the film during contact with the polyanion (ALG) solution. In this step, the polycations are complexed with polyanions from the solution as soon as they reach the film/solution interface. These complexes form the new upper layer of the film. The amount of newly deposited material is thus directly proportional to the number of polycation chains diffusing "out of" the film during its contact with the polyanion solution. Moreover, the number of polycation macromolecular chains diffusing to the interface is proportional to the film thickness. So the thickness of film grows exponentially.

Figure 4C shows the FL spectra of TPE-CS/ALG multilayer films with bilayer number from 1 to 8. Different from the

conventional dyes, TPE-CS with AIE characteristic does not show any spectral shift in FL measurement. Moreover, the excellent exponential relationship between the FL intensity and the number of bilayers, which is in accordance with the thickness variation of multilayer films, provides solid evidence for its capacity to monitor the LBL self-assembly process.

Surface Morphology and Cell Adhesion

Figure 5 shows the surface topography of TPE-CS ended multilayer films with bilayer number of 1.5, 3.5 and 5.5. As assembly process goes on, the height and surface fluctuation of multilayer films change regularly. The RMS of 3μm×3μm area increases from 4.114 nm (1.5 bilayer) to 11.56 nm (5.5 bilayer). After the deposition of 1.5 bilayers, a homogeneous film can be observed and the surface becomes fully coated, indicating that under chosen condition polyelectrolyte deposition proceeds rapidly.

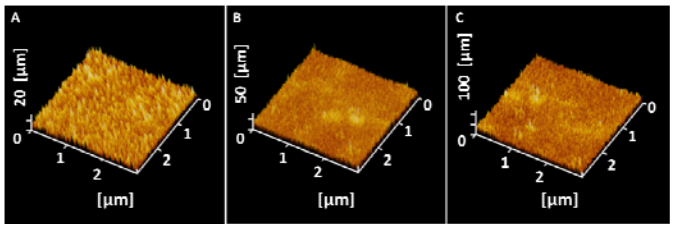

Figure 5 AFM images of (A) $(TPE\text{-}CS/ALG)_1/TPE\text{-}CS$, (B) $(TPE\text{-}CS/ALG)_3/TPE\text{-}CS$, (C) $(TPE\text{-}CS/ALG)_5/TPE\text{-}CS$ multilayer films.

Cell adhesion, spreading and migration on substrates are the first sequential reactions when contact with material surface, which is crucial for cell survival. The cellular behavior on biomaterials is an important factor for evaluation of the biocompatibility of biomaterial. Figure 6 shows the morphologies of 293T cells cultured on multilayer films with different layer numbers and different outermost layer. Cells randomly adhered and proliferated without preferred directions. Compared with the multilayer films with ALG as the outermost layer, cells attached on TPE-CS ended films had larger quantities and were fully spread.

Different outermost layer has different surface chemical composition, which may be the reason for the diverse cell adhesive behaviors. As the only positively charged polysaccharide in nature, CS is primarily responsible for electrostatic interactions with components of anionic glycosaminoglycans, proteoglycans and other negatively charged molecules in the cytomembrane, therefore CS has typically good cytocompatibility and shows to be more attractive for many kinds of cells to adhere[32-33]. On the contrary ALG-ended multilayer film with its negative surface charge and excessive hydrophilicity, presents cell anti-adhesion properties.

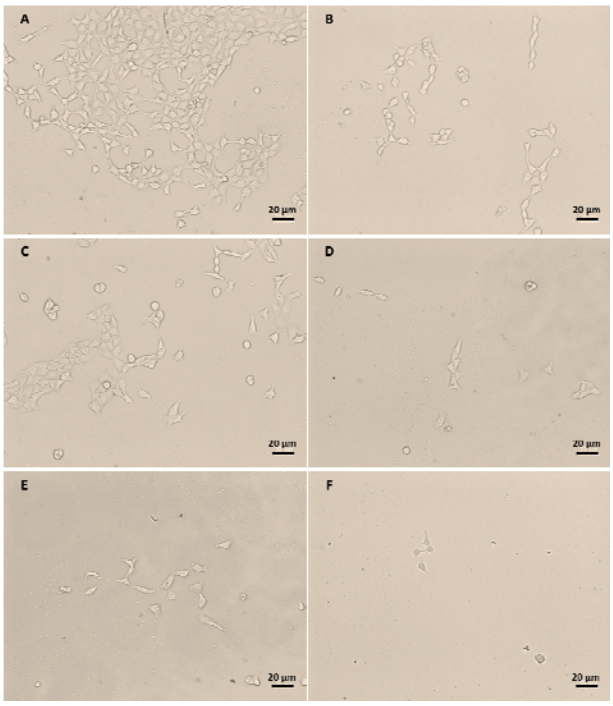

Figure 6 Microscopic observation of 293T cells cultured on (A) $(TPE\text{-}CS\ /ALG)_3/TPE\text{-}CS$, (B) $(TPE\text{-}CS\ /ALG)_4$, (C) $(TPE\text{-}CS\ /ALG)_5/TPE\text{-}CS$, (D) $(TPE\text{-}CS/ALG)_6$, (E) $(TPE\text{-}CS\ /ALG)_7/TPE\text{-}CS$, (F) $(TPE\text{-}CS\ /ALG)_8$ multilayer films after 3 d incubation.

For TPE-CS ended multilayer films with different layer numbers, cell adhesion decreases as the number of layers increases. These $(TPE\text{-}CS/ALG)_i$ multilayer films seem to have the same cell adhesion behavior as the (PLL/alginate) films described by Elbert *et al.*[34]. These authors attributed the "cell resistant" effect to the "gel-like" (PLL/alginate) films. Previous study also suggests that cell adhesion or cytophobicity is directly related to the swelling and hydrating properties of the polyelectrolyte multilayer films[35]. If the surface is highly hydrated, the cells will not attach accordingly. In the light of QCM results, the TPE-CS/ALG multilayer films are soft films swollen with water. Because of the exponential growth, films with layer number>3.5 tend to be much softer with considerable swelling capacity and may present water-rich hydrogel-like state in liquid phase environment, such as in vivo, resulting in the cell anti-adhesion property, which has great potential to be used to prevent tissue adhesion in biomedical application[36].

Conclusions

We have successfully synthesized the AIE-active TPE-CS bioconjugate as a FL probe (and also a polycation itself) to monitor its LBL self-assembly process with ALG. TPE-CS with AIE characteristic does not show any spectral shift in FL measurement. The FL intensity of the TPE-CS in the deposition films follows an excellent exponential relationship with the bilayer numbers in accordance with the thickness variation of multilayer films. At last, the cell adhesive properties of TPE-CS/ALG multilayer films were investigated. This novel CS-based AIE-active FL probe can be directly used to monitor multilayer deposition process, thus providing a new simple and convenient way for probing the LBL self-assembly of polycations and polyanions.

Acknowledgements

This work was financially supported by National Natural Science Foundation of China (Nos. 21104067, 21274127, 21374099 and 51473144), Key Basic Research Development Plan (973 Program) of China (Nos. 2009CB930104 and 2011CB606203), Fundamental Research Funds for the Central Universities (No.2013QNA4048) and Technology Foundation for Selected Overseas Scholar of Zhejiang Province.

Notes and references

[a]*MOE Key Laboratory of Macromolecular Synthesis and Functionalization, Department of Polymer Science and Engineering, Zhejiang University, Hangzhou 310027, China. E-mail: wangzk@zju.edu.cn; huql@zju.edu.cn.*

[b]*Department of Chemistry, Division of Biomedical Engineering, Institute for Advanced Study, and Institute of Molecular Functional Materials, The Hong Kong University of Science and Technology (HKUST), Clear Water Bay, Kowloon, Hong Kong, China. E-mail: tangbenz@ust.hk.*

1 M. M. Stevens and J. H. George, *Science*, 2005, ***310***, 1135-1138.
2 M. Tirrell, E. Kokkoli and M. Biesalski, *Surf Sci*, 2002, **500**, 61-83.
3 T. Boudou, T. Crouzier, K. Ren, G. Blin and C. Picart, *Adv Mater*, 2010, **22**, 441-467.
4 H. Ai, S. A. Jones and Y. M. Lvov, *Cell Biochem and Biophys*, 2003, **39**, 23-43.
5 P. Bertrand, A. Jonas, A. Laschewsky and R. Legras, *Macromol Rapid Comm*, 2000, **21**, 319-348.
6 X. Zhang, H. Chen and H. Zhang, *Chem Commun*, 2007, **14**, 1395-1405.
7 P. T. Hammond, *Adv Mater*, 2004, **16**, 1271-1293.
8 L. Richert, P. Lavalle, E. Payan, X. Z. Shu, G. D. Prestwich, J. F. Stoltz and C. Picart, *Langmuir*, 2004, **20**, 448-458.
9 N. M. Alves, C. Picart and J. F. Mano, *Macromol biosci*, 2009, **9,** 776-785.
10 G. V. Martins, E. G. Merino, J. F. Mano and N. M. Alves, *Macromol biosci*, 2010, **10**, 1444-1455.
11 E. S. Forzani, M. Otero, M. A. Pérez, M. L. Teijelo and E. J. Calvo, *Langmuir*, 2002, **18**, 4020-4029.
12 X. Zhang and J. Shen, *Adv Mater*, 1999, **11**, 1139-1143.
13 J. K. Jin, J. Z. Sun, Y. Q. Dong, H. P. Xu, W. Z. Yuan and B. Z. Tang, J *Lumin*, 2009, **129**, 19-23.
14 B. ZhongáTang and P. P. S. Lee, *J Mater Chem*, 2001, **11**, 2974-2978.
15 Y. Hong, J. W. Y. Lam and B. Z. Tang, *Chem Soc Rev*, 2011, **40**, 5361-5388.
16 Y. Hong, J. W. Y. Lam and B. Z. Tang, *Chem Commun*, 2009, **29**, 4332-4353.
17 E. L. Que, D. W. Domaille and C. J Chang, *Chem Rev*, 2008, **108**, 1517-1549.
18 M. S. T. Gonçalves, *Chem Rev*, 2008, **109**, 190-212.
19 A. Shao, Z. Guo, S. Zhu, S. Zhu, P. Shi, H. Tian and W. Zhu, *Chem Sci*, 2014, **5**, 1383-1389.
20 Y. Zhang, Y. Chen, X. Li, J. Zhang, J. Chen, B. Xu and W. Tian, *Polym Chem*, 2014, **5**, 3824-3830.
21 M. Gao, Q. Hu, G. Feng, B. Z. Tang and B. Liu, *J Mater Chem B*, 2014, **2**, 3438-3442.
22 Z. Zhao, B. Chen, J. Geng, Z. Chang, L. Aparicio-Ixta, H. Nie and B. Z. Tang, *Part Part Syst Char*, 2014, **31**, 481-491.
23 M. Wang, G. Zhang, D. Zhang, D. Zhu and B. Z. Tang, *J Mater Chem*, 2010, **20**, 1858-1867.
24 Z. Wang, S. Chen, J. W. Lam, W. Qin, R. T. Kwok, N. Xie and B. Z. Tang, *J Am Chem Soc*, 2013, **135**, 8238-8245.
25 G. V. Martins, J. F. Mano and N. M. Alves, *Carbohydrate Polym*, 2010, **80**, 570-573.
26 S. Boddohi, C. E. Killingsworth and M. J. Kipper, *Biomacromolecules*, 2008, **9**, 2021-2028.
27 G. Lawrie, I. Keen, B. Drew, A. Chandler-Temple, L. Rintoul, P. Fredericks and L. Grøndahl, *Biomacromolecules*, 2007, **8**, 2533-2541.
28 S. M. Notley, M. Eriksson and L. Wågberg, J *Colloid Inter Sci*, 2005, **292**, 29-37.
29 P. Lavalle, C. Picart, J. Mutterer, C. Gergely, H. Reiss, J. C. Voegel and P. Schaaf, *J Phys Chem B*, 2004, **108**, 635-648.
30 P. Lavalle, C. Gergely, F. J. G. Cuisinier, G. Decher, P. Schaaf, J. C. Voegel and C. Picart, *Macromolecules*, 2002, **35**, 4458-4465.
31 C. Picart, J. Mutterer, L. Richert, Y. Luo, G. D. Prestwich, P. Schaaf and P. Lavalle, *P Nati Acad Sci*, 2002, **99**, 12531-12535.
32 N. A. Peppas, J. Z. Hilt and A. Khademhosseini and R. Langer, *Adv Mater*, 2006, **18**, 1345-1360.
33 A. Di Martino, M. Sittinger and M. V. Risbud, *Biomaterials*, 2005, **26**, 5983-5990.
34 D. L. Elbert, C. B. Herbert and J. A. Hubbell, *Langmuir*, 1999, **15**, 5355-5362.
35 J. D. Mendelsohn, S. Y. Yang, J. A. Hiller, A. I. Hochbaum and M. F. Rubner, *Biomacromolecules*, 2003, **4**, 96-106.
36 X. L. Zhou, S. W. Chen, G. D. Liao, Z. J. Shen, Z. L. Zhang, L. Sun and X. D. Jin, *World J Gastroenterology*, 2007, **13**, 1262.

Graphical abstract

Monitoring Layer-by-layer Self-assembly Process of Natural Polyelectrolytes by Fluorescent Bioconjugate with Aggregation-induced Emission Characteristic

Jingwei Jia, Zhengke Wang*, Wentao Lu, Ling Yang, Qingwen Wu, Wei Qin, Qiaoling Hu*, Ben Zhong Tang*

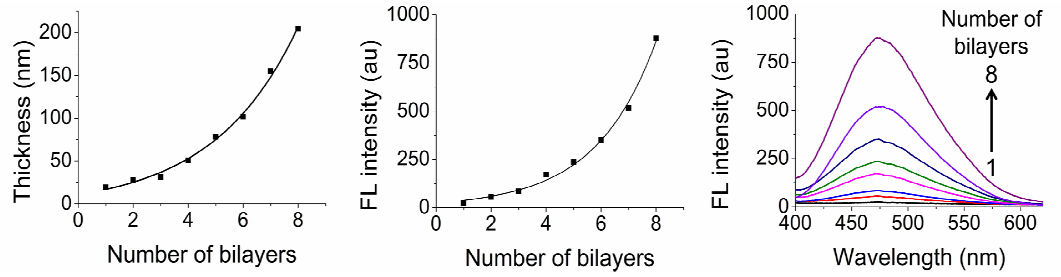

Exponential growth of multilayer films was monitored by fluorescence spectra using aggregation-induced-emission fluorogens, which is in accordance with ellipsometry results.